

Received Date : 06-Jul-2012
Revised Date : 29-Oct-2012
Accepted Date : 02-Nov-2012
Article type : Original Article

Functional specialization of duplicated *AP3*-like genes in *Medicago truncatula*

Edelín Roque¹, **Joanna Serwatowska**¹, **María Cruz Rochina**¹, **Jiangqi Wen**², **Kirankumar S. Mysore**², **Lynne Yenush**¹, **José Pío Beltrán**¹ & **Luis A. Cañas**¹

1. Instituto de Biología Molecular y Celular de Plantas (CSIC-UPV). Ciudad Politécnica de la Innovación, Edf. 8E. C/ Ingeniero Fausto Elio s/n. E-46011 Valencia. Spain
2. Plant Biology Division. The Samuel Roberts Noble Foundation. 2510 Sam Noble Parkway, Ardmore, OK 73401.USA

Correspondence to:

Luis A. Cañas
Telephone: +34 96 3877870
Fax: +34 96 3877859
Email: lcanas@ibmcp.upv.es

SUMMARY

The B-class of MADS-box genes has been studied in a wide range of plant species, but it has remained largely uncharacterized in legumes. Here we investigate the evolutionary fate of the duplicated *AP3*-like genes of a legume species. To gain insight into the extent to which B-class MADS-box gene functions are conserved or have diversified in legumes, we have isolated and characterized the two members of the *AP3* lineage in *Medicago truncatula*: *MtNMH7* and *MtTM6* (*euAP3* and *paleoAP3* genes respectively). A non-overlapping and complementary expression pattern of both genes is observed in petals and stamens. *MtTM6* was expressed predominantly in the outer cell layers of both floral organs and *MtNMH7* in the inner cell layers of petals and stamens. Functional analyses by reverse genetics approaches (RNAi and *Tnt1* mutagenesis) showed that the relative contribution of *MtNMH7* to petal identity is more important than that of *MtTM6*, whereas *MtTM6* plays a more important role in stamen identity than its paralog *MtNMH7*. Our results suggest that the *M. truncatula* *AP3*-like genes have undergone a functional specialization process associated to a complete partitioning of gene expression patterns of the ancestral gene lineage. We provide information regarding the similarities and differences in petal and stamen development among core eudicots.

Keywords: *AP3*-like genes, MADS-box, floral organ identity, legumes, *Medicago truncatula*, gene duplication, subfunctionalization, evolutionary fate.

Running Head: Functional specialization of *AP3*-like genes in *Medicago truncatula*

GenBank accession numbers: *MtTM6*: JN412097; *MsTM6*: JN412100; *PsTM6*: JN412098; *MtNMH7*: JN412096; *PsNMH7*: JN412099

This article has been accepted for publication and undergone full peer review but has not been through the copyediting, typesetting, pagination and proofreading process which may lead to differences between this version and the Version of Record. Please cite this article as an 'Accepted Article', doi: 10.1111/tpj.12068

© 2012 The Authors. The Plant Journal © 2012 Blackwell Publishing Ltd

Accepted Article

INTRODUCTION

Our understanding of the molecular mechanisms controlling the genetic regulation of flower development rests largely on genetic analyses carried out in the core eudicot species *Arabidopsis thaliana* and *Antirrhinum majus*. These studies have led to the ABC model (Bowman *et al.*, 1989; Coen and Meyerowitz, 1991). However, additional information is emerging regarding the identification of candidate genes that control floral organ identity in other angiosperms, including legumes (Baum *et al.*, 2002; Hecht *et al.*, 2005; Irish, 2006; Theissen and Melzer, 2007; Soltis *et al.*, 2009).

According to the ABC model, the combination of B and A-function genes specify petal identity in the second floral whorl, whereas the combination of B and C-function genes control stamen identity in the third whorl. A pair of MADS-box genes, *APETALA3* (*AP3*) and *PISTILLATA* (*PI*), encode the B-function activity in *A. thaliana* and *DEFICIENS* (*DEF*) and *GLOBOSA* (*GLO*) in *A. majus*. Mutations in either one of these genes produce transformations of petals into sepals and stamens into carpels (Bowman *et al.*, 1989; Sommer *et al.*, 1990; Schwarz-Sommer *et al.*, 1992; Tröbner *et al.*, 1992; Goto and Meyerowitz, 1994; Jack *et al.*, 1994).

Phylogenetic analysis of B-class MADS-box genes from representatives of all major lineages of angiosperms shows the high frequency of gene duplications within both *AP3* and *PI* lineages (Kramer *et al.*, 1998; Kramer and Irish, 2000; Becker *et al.*, 2002; Kramer *et al.*, 2003; Aoki *et al.*, 2004; Kim *et al.*, 2004; Stellari *et al.*, 2004). The ancestral gene of the *AP3/PI* lineages is thought to have undergone a duplication event yielding *AP3* and *PI* lineages before the diversification of the angiosperms (Aoki *et al.*, 2004; Kim *et al.*, 2004; Stellari *et al.*, 2004). Subsequently, the *AP3* lineage underwent another major duplication at the base of the core eudicots, giving rise to two *AP3*-like lineages: one termed *euAP3* that contains *AP3* itself and another lineage named *TM6*, which lacks a representative in *A. thaliana*, although it is present in many other eudicot taxa (Kramer *et al.*, 1998, Kramer *et al.*, 2006).

Duplicated genes are generally considered to adopt one of three possible fates: nonfunctionalization, in which one copy is silenced, neofunctionalization, in which one copy acquires an entirely new function whereas the other copy maintains the original function (Ohno 1970; Force *et al.*, 1999) and subfunctionalization, in which each descendant copy adopts part of the function of the ancestral gene (Hughes 1994; Force *et al.*, 1999; Lynch and Force 2000; Lynch *et al.*, 2001).

Most of the studies proposing a cause-effect relationship between gene duplication and functional divergence and evolution rely on phylogenetic analysis and expression patterns of duplicated genes. Thus, in many of these cases, functional studies are missing. However, studies conducted using different members of the Solanaceae, showed the subfunctionalization of duplicated genes in the *AP3* lineages, with *euAP3*-type genes evolving to play a primary role in petal and stamen development, whereas *TM6*-type genes have a partially overlapping function in stamen development

(Vandenbussche *et al.*, 2004; de Martino *et al.*, 2006; Geuten and Irish, 2010; Liu *et al.*, 2004). Recently, *AP3*-like genes have been functionally characterized in *Gerbera hybrida*, and were shown to play similar roles as their orthologous genes in *Petunia hybrida*, *Solanum lycopersicum* and *N. benthamiana* (Broholm *et al.*, 2010).

Flowers of model dicot species, such as *A. thaliana* or *A. majus*, form the primordia of petals and stamens independently, but in some legumes, including *M. truncatula*, these organs derive from special structures called common primordia that probably represent an evolutionary specialization. These structures are four ephemeral meristems that develop between sepal and carpel primordia and upon division each follows a characteristic pattern to produce the petal and stamen primordia (Ferrándiz *et al.*, 1999; Benlloch *et al.*, 2003; Tucker, 2003). B-class genes have been suggested to contribute to the control of the identity and determinacy of common primordia in legumes (Ferrándiz *et al.*, 1999; Taylor *et al.*, 2001; Berbel *et al.*, 2005) but experimental data are required to reinforce this hypothesis.

We report here the existence of two duplicated *AP3*-like genes in *M. truncatula* (an *euAP3* named *MtNMH7* and a *paleoAP3* named *MtTM6*). To shed light on the specific contribution of these paralogous genes to the control of petal and stamen identity we investigated their detailed expression pattern and we used reverse genetics approaches to uncover the function of these genes in legumes. We show that the duplicated *AP3*-like genes in this legume species control petal and stamen identity. Our results suggest that the *MtNMH7* and *MtTM6* paralogous genes have undergone a post-duplication subfunctionalization process, associated to a complete partitioning of gene expression patterns of the ancestral gene lineage.

RESULTS

Two Medicago truncatula AP3-like genes

We previously isolated and functionally analyzed two *M. truncatula* B-class MADS-box genes belonging to the *PI/GLO* subfamily (Benlloch *et al.*, 2009). With the aim to isolate the other B-class MADS-box genes involved in the control of petal and stamen identity in the *M. truncatula* flower, we have screened a floral cDNA library using the MADS-box fragment of the *A. majus DEFICIENS* gene as a probe. Eight of the isolated clones showed significant similarity to the *AP3* gene from *A. thaliana* (56% amino acid identity) and the other seven clones were similar to the *TM6* gene from tomato (59% amino acid identity). The obtained sequences were named *M. truncatula TM6* (*MtTM6*; GenBank accession n.: JN412097) based on its similarity with the *TOMATO MADS BOX GENE6* (*TM6*; Pnueli *et al.*, 1991) and *M. truncatula NMH7* (*MtNMH7*; GenBank accession n.: JN412096) according to its homology with the *AP3*-orthologue in *M. sativa* (*NMH7*).

The longest *MtTM6* cDNA clone was 1135 bp long and contained a 696 nt open reading-frame encoding a 232 amino acid protein. The longest *MtNMH7* cDNA clone was 984 nt long and contained a 687 bp open reading-frame encoding a 229 amino acid protein. The *MtTM6* genomic sequence indicates that the *MtTM6* gene is organized in seven exons (188, 70, 62, 109, 42, 45, 183 bp) and six introns (Figure S1a), and that *MtNMH7* is organized similarly with seven exons (188, 67, 63, 99, 42, 46, 185 bp) and six introns. These sequences were used as blastn queries, and displayed using Chromosome Visualization Tool (CViT blast: <http://www.medicago.org>). The *MtTM6* gene is located on chromosome 5 in the *M. truncatula* bacterial artificial chromosome AC136451, clone mth2-17d19 (Figure S1b), and the *MtNMH7* gene is located on chromosome 3 in the *M. truncatula* bacterial artificial chromosome AC151483, clone mth2-157f20 (Figure S1c). Both genes are present as a single-copy as confirmed by Southern blot analysis (Figure S3).

Alignments of the inferred amino acid sequences with selected AP3 orthologs showed that MtTM6 and MtNMH7 show all the common domains of a MADS-box MIKC type protein and the PI-derived motif (consensus FxFRLQPSQPNLH; Kramer *et al.*, 1998; Lamb and Irish, 2003). Moreover, MtTM6 shows the characteristic ancestral paleoAP3 motif in the C-terminal region, while MtNMH7 shows the euAP3 motif. Each of these motifs is highly conserved within lineages (Figure S2a and S2b).

Phylogenetic analysis reveals an ancient duplication in the ancestral gene of the M. truncatula AP3 lineage

To analyze the duplication event of the *M. truncatula* AP3-like genes in the context of time, we inferred the phylogeny using a nucleotide data set containing AP3 homologues from a wide variety of species (Table S1). We included “B gene” (*GGM2*-like) sequences isolated from diverse gymnosperms, AP3-like genes from basal angiosperms, magnoliids, monocots, early-divergent eudicots and core eudicots. In agreement with previous analyses (Kim *et al.*, 2004; Kramer *et al.*, 1998), we observed two major core eudicot lineages (euAP3 and TM6) derived from the ancestral paleoAP3 lineage. The topology of the phylogenetic tree confirms that the *M. truncatula* paralogs isolated here fall within the clade of the AP3-like genes, and that both *MtNMH7* and *MtTM6* can be specifically placed within their respective lineages, euAP3 and TM6. Based on the interpretation of the current phylogeny, the duplication resulting in the paralogs *MtNMH7* and *MtTM6* occurred early, coinciding with the base of the core eudicot radiation (Figure 1).

Complementary expression patterns between AP3-like genes in M. truncatula

Northern blot and qRT-PCR analyses revealed that both genes were expressed exclusively in floral tissues but with different expression levels (Figure 2). We did not detect any expression in root nodules, in contrast to what has been described previously for other AP3-like genes from legume species such as *Medicago sativa* and *Glycine max* (Heard and Dunn, 1995; Wu *et al.*, 2006; Páez-Valencia *et al.*, 2008).

In situ hybridization analysis during early stages of floral development showed that the *M. truncatula* AP3-like genes have non-overlapping expression patterns in the second and third floral whorls. *MtTM6* transcripts were initially detected at the centre of the floral meristem at stage 2 of floral development (Benloch *et al.*, 2003), whereas *MtNMH7* was not detected at this stage. At stage 4, expression of both genes can be observed in the common primordia that differentiate into petal and stamen primordia. Remarkably, we observed a complementary expression pattern at the cellular level at this early developmental stage: *MtTM6* transcripts were strongly detected in the outer cell layers that surround the common primordia, whereas *MtNMH7* transcripts were located in the inner cell layers of the common primordia (Figure 3a and e). This differential expression pattern persisted throughout the development of petals and stamens until complete flower development (Figure 3b, c, d, f and g). At late stages, *MtNMH7* expression was also detected in the ovules (Figure 3d), while *MtTM6* continues to be expressed in the outer cell layers of both floral organs (Figure 3h).

Protein-protein interactions of the *M. truncatula* B-class MADS-box proteins

The maintenance of AP3 and PI expression depends upon the interaction of both gene products (heterodimers) as part of larger MADS-box protein complexes (Riechmann *et al.*, 1996; and references therein).

We previously reported the expression pattern and the functional analysis of the two PI-like genes of *M. truncatula* (Benloch *et al.*, 2009). *MtPI* expression was detected at high levels in flowers, whereas *MtNGL9* expression was detected at very low levels in flowers and in all tissues analyzed, being slightly higher in nodules and leaves. We have retested the expression pattern of the two *M. truncatula* PI paralogs in inflorescence apices and we have found that *MtNGL9* is weakly expressed in the floral meristem in the cells that give rise to common petal-stamen primordia and later on during the development of petals and stamens. Moreover, *MtNGL9* mRNA was also detected in ovules (Roque *et al.*, unpublished).

To test the ability of the gene products to interact *in vitro*, we studied protein-protein interactions among the four *M. truncatula* B-class MADS box products in pairwise combinations using the yeast two-hybrid system (Figure 4). We found that both MtNMH7 and MtTM6 were able to interact with MtPI. In contrast to MtNMH7, which has heterodimerization capability with both PI-proteins, MtTM6 was able to interact with MtPI. Interestingly we observed homodimerization only in the case of MtPI. Further studies are in progress to quantitatively compare these protein-protein interactions and to confirm them *in planta*.

Loss-of-function analyses of *MtNMH7* and *MtTM6*

To assess the functional roles of AP3-like genes in *M. truncatula*, we used two reverse genetic approaches: RNAi gene silencing in stably transformed plants and *Tnt1* retrotransposon insertion in the *MtTM6* gene (Tadege *et al.*, 2008; Cheng *et al.*, 2011).

For RNAi silencing of *MtNMH7*, we generated a hairpin RNAi construct, with the C-terminal region of the *MtNMH7* cDNA (326-734 from ATG), and transformed *M. truncatula* cv. 2HA plants with this construct.

Flowers of the 35S::RNAi-*MtNMH7* plants with strong phenotypes (lines Tr13 and Tr14) displayed apparent morphological alterations (Figure 5b). The yellow petals in the 2nd whorl (W2) showed patches of green tissue. The midveins of the standard or *vexillum* (V) became broader and greener, especially toward the edge of the corolla, and wings (W) and keel (K) petals also showed green patches. In some cases, the green tissue included almost the whole petal, and in others, the green tissue was present only at the border of petals (Figure 5b, white arrows). In the 3rd whorl (W3), most of the stamens were able to differentiate the staminal tube and anthers. However, the anthers fail to produce pollen grains. Moreover, the filaments of the two stamens flanking the staminal tube were green and contained trichomes and the anthers had lost their characteristic morphology, suggesting that reduction of *MtNMH7* expression causes slight stamen carpelloidy (Figure 5b, white arrows). These transformations were more evident at the cellular level, with adaxial W2 cells showing sepaloïd characteristics. The typical conical epidermal cells present in the wild type petals (Figure 6a) were replaced by stomata-containing sepal-like epidermal cells, indicating a shift of petal toward sepal identity in the green petal patches (Figure 6b and c). Cells of the 35S::RNAi-*MtNMH7* carpelloïd stamens flanking the staminal tube (Figure 6g and 6o) had lost their narrow and longitudinally elongated morphology, typical of a wild type anther filament (Figure 6e), and now resembled the cells present in the middle wild-type carpel with the presence of trichomes (Figure 6f). Moreover, the characteristic irregular epidermal cells found in wild type anthers (Figure 6i) were replaced by cells quite similar to those present at the wild-type ovule surface in the anthers of 35S::RNAi-*MtNMH7* flowers (Figure 6j). This change can be observed in Figure 6k. In summary, reduction in *MtNMH7* expression resulted in a partial homeotic transformation of petals into sepal-like mosaic organs and a slight homeotic conversion of stamens into carpelloïd organs. These phenotypic changes indicate that *MtNMH7* is involved in petal and stamen development, but its reduced expression is not sufficient to completely abolish the B function.

The transcript level of *MtNMH7* in 35S::RNAi-*MtNMH7* plants was considerably reduced (15% of wild-type level) although not completely eliminated (Figure S4), whereas the expression levels of *MtTM6* and *MtNGL9* were similar to the wild-type. Also, the *MtPI* expression was reduced 30%. These results indicate that *MtNMH7* could be required only to maintain full *MtPI* expression without affecting *MtNGL9* or *MtTM6* expression or, alternatively, that 15% of the total *MtNMH7* expression could be sufficient to directly or indirectly maintain *MtNGL9* and *MtTM6* expression, but not to fully maintain *MtPI* expression levels.

To elucidate the function of *MtTM6*, we used both RNAi silencing and *Tnt1* insertion approaches. For RNAi silencing of *MtTM6*, we generated a hairpin RNAi construct with the C-terminal region of *MtTM6* cDNA (444-716 from ATG), and transformed *M. truncatula* cv. R108 plants. The

mttm6-1 Tnt1 insertion allele was identified as described in the experimental procedures. The *Tnt1* insertion lies at the position 105 of the first exon of *MtTM6*.

The *mttm6-1* flowers (Figure 5c) showed a stronger loss-of-B-function phenotype than the 35S::RNAi-*MtTM6* flowers (Figure 5d). The petals in the *mttm6-1* flowers resulted in small patches of green tissue at the borders and, in some cases, a carpel-like structure fused to the edge of the petal (Figure 5c, arrows). The 35S::RNAi-*MtTM6* petals exhibited defects only in their shape. Reduction in *MtTM6* expression resulted in some stamens differentiating into filaments and anthers that fail to produce pollen grains. Other stamens failed to develop anthers, producing stigma-like structures in their place (Figure 5d, white arrow). The filaments were green with some trichomes (Figure 5d). However, total loss of *MtTM6* expression caused an almost full conversion of all anthers into carpels. These were broader and greener than wild-type anthers and displayed typical carpel trichomes on their surface (Figure 5c).

Scanning electron microscopy (SEM) of the border of the second whorl petals in *mttm6-1* plants revealed a conversion of the conical epidermal cells (Figure 6a) into stomata-containing sepal-like epidermal cells (Figure 6b), suggesting a shift of identity from petal towards sepal in this petal part (Figure 6d).

mttm6-1 flowers never developed the staminal tube. Instead, green carpelloid-like structures with trichomes at their surface were formed (Figures 5c and 6q). A closer look showed that while the epidermis of wild-type filaments is constituted by narrow and longitudinally elongated cells (Figure 6e), the cell types in the *mttm6-1* third whorl organs resembled the cells present in the low and middle wild-type carpel (Figure 6f), which develop trichomes (Figure 6h).

Whereas the cells in the wild-type anthers displayed their typical irregular shape (Figure 6i), the *mttm6-1* anthers contain cells similar to those present at the end of the wild type carpel, in the region most proximal to the stigma (Figure 6l). This transformation can be observed in Figure 6h.

We analyzed the expression of the *M. truncatula* B-class MADS box genes in the 35S::RNAi-*MtTM6* (line Tr1) and *mttm6-1* plants by qRT-PCR. The RNAi line showed reduced *MtTM6* expression (20% of the wild-type level), and all the other B class genes showed reduced expression levels when compared to the wild-type level (Figure S4). Similar results were observed for the *mttm6-1* line, where the *MtTM6* expression disappeared completely as consequence of the *Tnt1* insertion in the *MtTM6* gene (Figure S4). These results suggest that the expression of *MtTM6* is required to maintain the expression of the other *M. truncatula* B-class genes.

DISCUSSION

B-class MADS-box genes have been implicated in the regulation of floral organ identity in the second (petals) and third (stamens) whorls in angiosperms. Recent functional analysis and expression pattern studies of the *AP3* and *PI* lineages have demonstrated that in various instances these genes could

have swapped roles, retained or lost the ancestral ones or acquired novel functions. The multiple gene duplication events within both lineages have led to sub- and non-functionalization in some cases, processes often associated with changes in expression patterns (Vandenbussche *et al.*, 2004; de Martino *et al.*, 2006; Rijpkema *et al.*, 2006; Drea *et al.*, 2007).

Functional specialization of *M. truncatula* AP3-like genes

We have generated RNAi-induced *MtTM6* and *MtNMH7* loss-of-function transgenic plants and identified a complete *MtTM6* loss-of-function insertional (*Tnt1*) mutation. This functional analysis uncovered interesting aspects of the regulatory control of petal and stamen development in this legume species.

The RNAi-induced loss-of-*MtNMH7* function results in defects predominantly in petal development. The 35S::RNAi-*MtNMH7* plants showed a partial conversion of petals into sepaloid structures, identifying petals with patches of green tissue and sepal-like cells, whereas the stamens were weakly transformed into carpel-like organs. Changes in epidermal cell types of petal and stamens could be explained by protein movement from the inner cells, where the *MtNMH7* gene is expressed, to external cell layers. Usually the mRNA and the MADS-box protein co-localize in the same cells or tissues but it is known from studies on the B-class genes *DEF* and *GLOB* from *A. majus* (Perbal *et al.*, 1996) that particular MADS domain transcription factors are able to transfer from one cell to another, where they may have a non-cell-autonomous function. Urbanus *et al.* (2009) unravelled the *in planta* protein localization patterns of four MADS domain proteins and reported that discrepancies between mRNA and protein patterns occasionally observed may suggest a possible non-cell autonomous action of these factors by intercellular transport via plasmodesmata or alternative control mechanisms. In *MtNMH7*-RNAi loss-of-function flowers, *MtPI* expression was reduced, suggesting that *MtNMH7* positively regulates *MtPI*. Alternatively, a low level of *MtNMH7* could be sufficient for autoregulation and to directly or indirectly maintain *MtNGL9* and *MtTM6* expression, but it could be insufficient to maintain the *MtPI* expression level. If the protein-protein interactions detected reflect the ones produced *in vivo*, the MtTM6/MtPI heterodimeric complex would be the most abundant B-class protein complex that could be formed in the 35S::RNAi-*MtNMH7* line. Taking into account the low-level of *MtNMH7* expression in this line, other complexes (MtNMH7/MtNGL9; MtNMH7/MtPI) might be formed, but they would be insufficient to confer petal identity, indicating the importance of *MtNMH7* in petal identity specification. Therefore, MtTM6/MtPI would be sufficient to confer almost full stamen identity but would be insufficient to confer the complete petal identity.

In contrast, the *mttm6-1* mutant and the RNAi-induced loss-of-*MtTM6* function plants produce flowers displaying homeotic transformations predominantly in the third whorl. Down-regulation of *MtTM6* activity in 35S::RNAi-*MtTM6* plants did not produce homeotic defects in petal development. The only phenotypic effect that we observed was a change in petal shape. The lack of homeotic conversions in petals would be the result of low-level residual expression of *MtTM6* in these lines as

deduced from the comparison of the phenotypes of *MtTM6*-RNAi and *mttm6-1* lines. Similarly, de Martino *et al.* (2006), after phenotypic analysis of tomato *TM6*-RNAi transgenic lines, were not able to exclude the possibility that the lack of a homeotic phenotype in petals was the result of low-level residual expression of *TM6* in these lines. *mttm6-1* plants show almost full conversion of stamens into carpels, and a weak homeotic conversion of petals into sepal-like organs. In both 35S::RNAi-*MtTM6* and *mttm6-1* flowers, all the B-class genes showed reduced expression when compared with the wild-type levels (Figure S4), suggesting that MtTM6 positively regulates all the three other B-class genes. In *mttm6*, where the stamens are almost fully replaced by carpels, two heterodimers would be hypothetically active: MtNMH7/MtPI and MtNMH7/MtNGL9. Both complexes would be sufficient to confer almost full petal identity, but in contrast they would be not sufficient to confer stamen identity.

MtNMH7 and *MtTM6* appear to regulate the other B-class genes at the transcriptional level. Their expression could be required directly or indirectly (perhaps via larger multimeric MADS-box protein complexes) in the auto and cross-regulatory loop, in which the formation of a heterodimer between PI/GLO and AP3/DEF members could be required to maintain the expression of the *M. truncatula* B-class genes in petals and stamens (Riechmann *et al.*, 1996).

Based on the protein interaction data, the expression patterns of B-class genes in RNAi or *Tnt1* lines, as well as the phenotypical differences of individual *MtNMH7* or *MtTM6* loss-of-function plants, we conclude that both AP3-like genes are necessary for petal and stamen identity. *MtNMH7* appears to play a major role in determining petal identity, whereas *MtTM6* appears to do the same with respect to stamen identity. Even so, both genes are implicated in second and third whorl specification.

Differences in expression patterns of duplicated M. truncatula AP3-like genes can partially explain their functional specialization

Few studies have investigated the functional divergence process related to duplicated AP3-like genes in the core eudicot species. Data concerning functional analyses of the AP3-like genes are available in *Petunia hybrida* (*PhDEF* and *PhTM6*), *Solanum lycopersicum* (*TAP3* and *TM6*), *Nicotiana benthamiana* (*NbDEF* and *NbTM6*) and *Gerbera hybrida* (*GDEF2* and *GDEF1*) (Vandenbussche *et al.*, 2004; Rijpkema *et al.*, 2006; de Martino *et al.* 2006; Geuten and Irish, 2010 ; Broholm *et al.*, 2010). *eu-AP3*-like genes from these species show similar expression patterns during petal and stamen development, and their loss-of-function phenotypes in tomato (*TAP3*) and Nicotiana (*NbDEF*) are quite similar, displaying marked homeotic conversions of petal into sepals and stamens into carpelloid structures (Liu *et al.*, 2004; de Martino *et al.*, 2006; Geuten and Irish, 2010). In Gerbera, the downregulation of *GDEF2* also causes changes in whorl 2 and 3 (Broholm *et al.*, 2010). Unlike *euAP3*-like genes, some *TM6*-like genes as *PhTM6*, *NbTM6* and *GDEF1* are initially expressed in the four floral organs (Vandenbussche *et al.*, 2004; Geuten and Irish, 2010 ; Broholm *et al.*, 2010), while *TM6* is expressed throughout the three inner whorls (de Martino *et al.*, 2006). Expression of *TM6*-like

genes becomes predominant in stamens, but at later stages they are strongly expressed in the developing carpel and in stamens (Vandenbussche *et al.*, 2004; de Martino *et al.*, 2006; Geuten and Irish, 2010; Broholm *et al.*, 2010). The suppression of *TM6* orthologs is qualitatively different. Loss-of-function of *TM6* and *GDEF1* produces flowers with weak conversion of stamens into carpels (de Martino *et al.*, 2006; Broholm *et al.*, 2010). *Nicotiana* transgenic plants, in which *NbTM6* expression was suppressed, reveal weakly homeotic transformations of stamens into carpelloid structures and also weak defects in petals and ovules (Geuten and Irish, 2010), while loss-of-function of *PhTM6* has no obvious phenotype (Rijpkema *et al.*, 2006), suggesting different degrees of functional redundancy of *TM6*-like genes in stamen identity with their respective *eu-AP3* genes.

MtNMH7 and *MtTM6* are expressed in the regions of the floral meristem that give rise to petal and stamens (common primordia) and their expression in these floral organs persist until later stages of development. At early developmental stages, *MtTM6* expression was also observed in the central region of floral meristem, but we did not observe expression of *MtTM6* outside the second and third whorls at later developmental stages, in contrast to the expression of their *TM6*-like orthologs. Moreover, *MtNMH7* is expressed in ovules at later stages of development, an expression pattern that could be characteristic of legumes since in soybean (*Glycine max*) the floral expression of the *euAP3* gene *GmNMH7* was also observed in fully differentiated carpel and ovules (Wu *et al.*, 2006). *MtNMH7* and *MtTM6* genes appear to be expressed at different levels and with a mutually antagonistic expression pattern in different subpopulations of cells within petals and stamens. The *MtTM6* transcript was strongly expressed in the outer cell layers that surround the second and third whorls, whereas *MtNMH7* was expressed inside them. Our results suggest that the coordinated expression of B-class genes in the inner cell layers of the organ primordia plays an important role in specifying petal identity, while their expression in the outer cell layers could be mainly required to specify stamen identity. In agreement with this complementary expression pattern, *MtTM6* and *MtNMH7* do not seem to have any degree of functional redundancy as described for their orthologs in *Petunia*, tomato, *Nicotiana* or *Gerbera*. These observations suggest that regulatory changes play prominent roles in the diversification of their functions. *MtNMH7* and *MtTM6* could have experienced a subfunctionalization process, concomitant with a complete partitioning of the expression pattern of the ancestral gene lineage.

Our results provide information on the similarities and differences in petal and stamen development between core eudicots and we also show evidence regarding the evolutionary fate of the duplicated *AP3*-like genes of a legume species, where the B-function MADS-box genes had remained largely uncharacterized.

EXPERIMENTAL PROCEDURES

Plant material

Medicago truncatula cv. Jemalong lines A17 and R108, *Medicago sativa* cv. RSY-27 and *Pisum sativum* cv. Alaska plants were used in this study. Plants were grown in the greenhouse, at 22°C

(day) and 18°C (night) with a 16 h light / 8 h dark photoperiod, in a mixture of soil:sand (3:1) irrigated with Hoagland N^o.1 solution supplemented with oligoelements (Hewitt, 1966).

Identification of *Tnt1* insertion sites in *MtTM6* and co-segregation test

M. truncatula R108 was transformed with a construct containing the complete *Tnt1* retroelement of tobacco as described previously (d'Erfurth *et al.*, 2003). *Tnt1* tagging was carried out using one of these transgenic lines (Tnk7-7) to activate *Tnt1* transposition. Mutagenized plants that contain multiple independent *Tnt1* inserts were regenerated from leaf explants of the starter line as described (Tadege *et al.*, 2005, 2008; Cheng *et al.*, 2011). The *mttm6-1* allele was identified by screening of a segregating population of approximately 9000 independent R1 lines. For pooled DNA screening, we used primers based on the *MtTM6* sequence (MtTM6 F and MtTM6-F1; Table S2) in combination with primers from both sides of the *Tnt1* long-terminal repeats (Tnt1-F, Tnt1-F1, Tnt1-R and Tnt1-R1; Table S2). PCR was performed using genomic DNA pools from 9000 *Tnt1*-carrying transgenic plants (Cheng *et al.*, 2011). A PCR product of 750 bp was obtained from one of these pools using the combination of MtTM6-F and Tnt1-F. One part of the PCR product corresponds to the first 105 bp of the coding sequence of the *MtTM6* gene. The rest of the amplified sequence corresponds to the border of the LTRs of the *Tnt1*. We confirmed that the amplified fragment represents an insertion of the retrotransposon into the *M. truncatula MtTM6* gene (Figure S1a). Fifteen T2 plants from the NF1297 line were grown in the greenhouse and their phenotype was analyzed. Three plants of this population exhibited the *mttm6-1* mutant phenotype. PCR analysis was performed in plants showing WT phenotype using primer combinations MtTM6-F / Tnt1-F and MtTM6-F / MtTM6-505 (Table S2) to distinguish heterozygous and wild-type plants. Heterozygous lines were self-pollinated and one line (NF1297-4) selected for further analysis. About one-fourth of the resultant progeny (5/22 plants) exhibited the floral phenotype previously and co-segregated with the *Tnt1* insertion.

Nodulation assay

Plant nodulation tests were performed in the greenhouse as described previously (Coronado *et al.*, 1995; Benlloch *et al.*, 2009).

Isolation of cDNA and genomic sequences of *MtNMH7* and *MtTM6* cDNAs. Sequence analysis

cDNAs were isolated from a library of *M. truncatula* A17 inflorescence apices (Benlloch *et al.*, 2006), using the MADS-box fragment of the *A. majus DEFICIENS* gene as a probe. Sequence alignments and similarity comparisons of the inferred proteins were performed using the MACVECTOR 9.5 software (MacVector, Inc.). The deduced amino acid sequence was aligned using the CLUSTALW tool in MACVECTOR 9.5. Genomic sequence of *MtNMH7* and *MtTM6* were obtained by PCR with genomic DNA as template using the primers MtNMH7-ATG and MtNMH7-766 and MtTM6-ATG and MtTM6-725 respectively (Table S2).

Isolation and sequence analysis of MsTM6, PsNMH7 and PsTM6 cDNAs

MsTM6, *PsNMH7* and *PsTM6* were obtained by RT-PCR and 3' RACE from *M. sativa* and *P. sativum* floral cDNA samples. *TM6*-like genes from alfalfa and pea were obtained with primers designed against the mRNA of the *M. truncatula MtTM6* gene (*MtTM6*-ATG and *MtTM6*-622; Table S2). The 3' untranslated regions (UTR) and C-terminal region were obtained using the 3' RACE System for Rapid Amplification of cDNA Ends (Invitrogen) with nested gene-specific primers *MsTM6*-362 and *PsTM6*-362 from the *M. sativa* and *P. sativum* floral cDNAs respectively (Table S2). The *euAP3*-like gene from *P. sativum* was obtained with primers designed against the mRNA for the *M. truncatula MtNMH7* gene (*MtNMH7*-ATG and *MtNMH7*-671; Table S2). The 3' UTR and C-terminal region were obtained using the 3' RACE System for Rapid Amplification of cDNA Ends (Invitrogen) with nested gene-specific primer *PsNMH7*-384 (Table S2) from the *P. sativum* floral cDNA. Sequence alignment and similarity comparisons of the inferred proteins were performed using the MACVECTOR 9.5 software (MacVector, Inc.). The deduced amino acid sequence was aligned using the CLUSTALW tool in MACVECTOR 9.5 and further refined by hand.

Phylogenetic tree

The phylogenetic tree was inferred by Neighbor-Joining using Poisson-Corrected amino acid distances. Reliability of internal nodes was assessed using bootstrap with 1000 pseudo-replicates. The tree was rooted using five *PI*-like sequences: *AtPI*, *AmGLO*, *NtGLO*, *PhGLO1* and *PhGLO2*. This choice was based on the fact that the *AP3* and *PI* are known to be paralogous lineages and are therefore each other's natural outgroups. Tree inference was conducted using *MEGA* version 5 (Tamura *et al.*, 2007). The data set comprised 74 previously reported *AP3*-like genes obtained from GenBank and 5 *AP3*-like sequences that are not found in GenBank. All sequences used in this analysis, with their GenBank accession numbers and respective species are included in Table S1.

Real Time RT-PCR analysis

Total RNA was isolated from roots, nodules and inflorescences from wild-type *M. truncatula* A17 plants and inflorescences from 35S::RNAi-*MtTM6*, 35S::RNAi-*MtNMH7* and *mttm6-1* plants, using the RNeasy Plant mini Kit (QIAGEN) according to the manufacturer's instructions. RNA samples were measured and equalised, their integrity was analyzed by gel electrophoresis. Total RNA was treated with *rDNaseI* of the *DNase* Treatment and Removal Kit (AMBION). Primers were designed for all genes from 3' end of the gene using PRIMER EXPRESS version 2.0 (Applied Biosystems) with default parameters. For First-strand synthesis, total RNA (1µg) was reverse-transcribed in a 20 µl reaction mixture using the PrimerScript 1st strand cDNA Synthesis Kit (TAKARA). One microliter of RT reaction was used for a Real Time RT-PCR analysis with 300 nM of each primer mixed with the Power SYBR[®] Green PCR Master Mix (Applied Biosystems) according to the manufacturer's instructions. The reaction was carried out into 96 well-optical reaction plates using an ABI PRISM 7500 Sequence Detection System and appropriate software (Applied Biosystems). The relative levels were determined by the 2^{-ΔΔCt} Method. To normalize the variance among samples, *Secret Agent*

(*O*-linked *N*-acetyl glucosamine transferase: TC77416; Hartweck *et al.*, 2002) was used as an endogenous control. All reactions were performed in triplicate using a biological replicate for each sample. The primers used were MtNGL9-qRTDIR and MtNGL9-qRTREV; MtPI-qRTDIR and MtPI-qRTREV; MtNMH7-qRTDIR and MtNMH7-qRTREV and MtTM6-qRTDIR and MtTM6-qRTREV; Sec.Ag-qRTDIR and Sec.Ag-qRTREV (Table S2).

Southern blot hybridization

Plant genomic DNA was extracted from leaves of *M. truncatula* A17 as described in Dellaporta *et al.* (1983). Ten micrograms of DNA were digested with *EcoRI*, *BamHI* and *HindIII*, separated on 0.7% Tris-acetate EDTA 1X agarose gels overnight at 1V/cm and transferred to a nylon membrane. Southern blot hybridization was performed by the standard method using two different conditions (52 and 65°C). cDNA probes were generated by PCR with the primers MtNMH7-289 and MtNMH7-734 and MtTM6-362 and MtTM6-698 (Table S2).

Two-Hybrid analysis

The B-class MADS-box transcription factors were subcloned into the *GAL4*-based two hybrid vectors, pGBD-C2 (James *et al.*, 1996) and pACT-2 (Clontech Lab. Inc.) and transformed into the PJ69-4A yeast strain (James *et al.*, 1996). Interactions between the transcription factors were tested by spotting a 1:200 dilution of each strain onto minimal media (SD) plates with the indicated supplements. In accordance with the genotype of the PJ69-4A strain, positive interactions are indicated by growth in media lacking histidine and adenine (SD-L-W-H-A). Identical results were observed for three independent transformants.

RNA in situ hybridization

RNA *in situ* hybridization with digoxigenin-labelled probes was performed on 8 µM longitudinal paraffin sections of *M. truncatula* inflorescences as described (Ferrándiz *et al.*, 2000). The RNA antisense and sense probes were generated with the T7 and SP6 polymerases respectively, using a 337-bp fragment of *MtTM6* (362-698 from ATG) and a 445-bp fragment of *MtNMH7* (289-734 from ATG) cloned into the pGEM-T easy vector (Promega).

Generation of transgenic plants

Transformation of *M. truncatula* R-108 was performed as described previously (d'Erfurth *et al.*, 2003). The 35S::RNAi-*MtNMH7* construct was made with the 326-bp fragment of *MtNMH7* (326-734 from ATG), amplified with the primers MtNMH7-DIR-RNAi and MtNMH7-REV-RNAi with incorporation of two restriction sites (underlined) used for cloning into the pHANNIBAL vector (Wesley *et al.*, 2001). The 35S::RNAi-*MtTM6* construct was made with the 278-bp fragment of *MtTM6* (444-716 from ATG), amplified with the oligonucleotides MtTM6-DIR-RNAi and MtTM6-REV RNAi (Table S2).

Northern blot analysis

Total RNA (15 µg) was isolated from frozen leaves, roots, root nodules, stems and flower buds by phenol-chlorophorm extraction and precipitated with 3M lithium chloride. RNA electrophoresis was carried out in formaldehyde-agarose gels, transferred to Hybond N⁺ membranes (Amersham Biosciences), and hybridized with ³²P-labeled probes under standard conditions. The probes used were: a 337-bp fragment of *MtTM6* (362-698 from ATG), amplified with the oligonucleotides MtTM6-362 and MtTM6-698 and a 445-bp fragment of *MtNMH7* (289-734 from ATG) amplified with MtNMH7-289 and MtNMH7-734 (Table S2).

Light microscopy and cryo-SEM

Light photographs of wild-type, 35S::RNAi-*MtTM6*; 35S::RNAi-*MtNMH7* and *MtTM6*-Tnt1(*mttm6-1*) flowers were made with a stereomicroscope Leica MZ28. For cryo-SEM, samples were frozen in slush nitrogen and attached to the specimen holder of a CT-1000C Cryo-transfer system (Oxford Instruments, UK) interfaced with a JEOL JSM-5410 scanning electron microscope. The samples were then transferred from cryostage to the microscope sample stage, where the condensed surface water was sublimed by controlled warming to -85°C. Afterwards, the sample was transferred again to the cryostage in order to gold coat it by sputtering. Finally the sample was put back on the microscope sample stage to be viewed at an accelerating voltage of 15 KeV.

ACKNOWLEDGEMENTS

This work was funded by grants BIO2006-09374 and BIO2009-08134 from the Spanish Ministry of Science and Innovation (MICINN). We are gratefully to Dr. Mario A. Fares and Dr. Santiago F. Elena (IBMCP, Valencia) for helpful comments and bioinformatics support. The collaboration and assistance of Rafael Martínez-Pardo in the greenhouse is gratefully acknowledged.

SUPPORTING INFORMATION

Figure S1: Schematic diagram of the Tnt1 insertion in the *MtTM6* gene and localization of the *MtTM6* and *MtNMH7* genes in the *M. truncatula* physical map.

Figure S2: Sequence analysis of *Medicago truncatula* AP3-like genes.

Figure S3: Southern blot analysis of *MtTM6* and *MtNMH7*.

Figure S4. Expression analysis of the *M. truncatula* AP3-like genes in *mttm6-1*, 35S::RNAi-*MtTM6* and 35S::RNAi-*MtNMH7* floral buds.

Table S1. Sequences of the AP3 and PI-like genes used in the phylogenetic analysis.

Table S2. Primers used in this work.

REFERENCES

- Angenent, G.C., Busscher, M., Franken, J., Dons, H.J.M. and van Tunen, A.J. (1995) Functional interaction between the homeotic genes *FBP1* and *pMADS1* during petunia floral organogenesis. *Plant Cell* **7**, 507-516.
- Aoki, S., Uehara, K., Imafuku, M., Hasebe, M. and Ito, M. (2004) Phylogeny and divergence of basal angiosperms inferred from *APETALA3*- and *PISTILLATA*-like MADS-box genes. *J. Plant Res.* **117**, 229–244.
- Baum, D.A., Doebley, J., Irish, V.F. and Kramer, E.M. (2002) Response: Missing links: the genetic architecture of flower and floral diversification. *Trends in Plant Science* **7**, 31-34.
- Becker, A., Winter, K-U., Meyer, B., Saedler, H. and Theissen, G. (2000) MADS-box gene diversity in seed plants 300 million years ago. *Mol. Biol. Evol.* **17**(10), 1425-1434.
- Becker, A., Kaufmann, K., Freialdenhoven, A., Vincent, C., Li, M.A., Saedler, H. and Theissen, G. (2002) A novel MADS-box gene subfamily with a sister-group relationship to class B floral homeotic genes. *Mol. Genet. Genomics* **266**, 942–950.
- Benlloch, R., Navarro, C., Beltrán, J.P. and Cañas, L.A. (2003) Floral development of the model legume *Medicago truncatula*: ontogeny studies as a tool to better characterize homeotic mutations. *Sexual Plant Reproduction* **15**, 231-241.
- Benlloch, R., d'Erfurth, I., Ferrándiz, C., Cosson, V., Beltrán, J.P., Cañas, L.A., Kondorosi, A., Madueño, F. and Ratet, P. (2006) Isolation of *mtpim* proves *Tnt1* a useful reverse genetics tool in *Medicago truncatula* and uncovers new aspects of AP1-like functions in legumes. *Plant Physiology* **142**, 972-983.
- Benlloch, R., Roque, E., Ferrándiz, C., Cosson, V., Caballero, T., Penmetsa, R.V., Beltrán, J.P., Cañas, L.A., Ratet, P. and Madueño, F. (2009) Analysis of B function in legumes: PISTILLATA proteins do not require the PI motif for floral organ development in *Medicago truncatula*. *Plant Journal* **60**, 102-111.
- Berbel, A., Navarro, C., Ferrándiz, C., Cañas, L.A., Beltrán, J.P. and Madueño, F. (2005) Functional conservation of *PISTILLATA* activity in a pea homolog lacking the PI motif. *Plant Physiology* **139**, 174-185.
- Bowman, J.L., Smyth, D.R. and Meyerowitz, E.M. (1989) Genes directing flower development in *Arabidopsis*. *Plant Cell* **1**, 37-52.
- Broholm, S.K., Pöllänen, E., Ruokolainen, S., Tähtiharnu, S., Kotilainen, M., Albert, V.A., Elomaa, P. and Teen, T.H. (2010) Functional characterization of B class MADS-box transcription factors in *Gerbera hybrida*. *Journal of Experimental Botany* **61**, 75-85.
- Coen, E.S. and Meyerowitz, E.M. (1991) The war of the whorls. Genetic interactions controlling flower development. *Nature* **353**, 31-37.
- Coronado, C., Zuanazzi, J.A.S., Sallaud, C., Quirion, J.-C., Esnault, R., Husson, H.-P., Kondorosi, A. and Ratet, P. (1995) Alfalfa root flavonoid production is nitrogen regulated. *Plant Physiol.* **108**, 533–542.
- Cheng, X., Wen, J., Tadege, M., Ratet, P. and Mysore, K.S. (2011) Reverse genetics in *Medicago truncatula* using *Tnt1* insertion mutants. *Methods Mol Biol.* **678**, 179-190.
- d'Erfurth, I., Cosson, V., Eschstruth, A., Lucas, H., Kondorosi, A. and Ratet, P. (2003) Efficient transposition of the *Tnt1* tobacco retrotransposon in the model legume *Medicago truncatula*. *Plant Journal* **34**, 95-106.
- de Martino, G., Pan, I., Emmanuel, E., Levy, A. and Irish, V.F. (2006) Functional analyses of two tomato *APETALA3* genes demonstrate diversification in their roles in regulating floral development. *Plant Cell* **18**, 1833-1845.
- Dellaporta, S.L., Wood, J., Hicks, J.B. (1983) A plant DNA miniprep: version II. *Plant Mol Biol Rep* **1**, 19–21.
- Drea, S., Hileman, L., de Martino, G. and Irish, V. (2007) Functional analyses of genetic pathways controlling petal specification in poppy. *Development* **134**, 4157-4166.
- Dong, Z.C., Zhao, Z., Liu, C.W., Luo, J.H., Yang, J., Huang, W.H., Hu, X.H., Wang, T.L. and Luo, D. (2005) Floral patterning in *Lotus japonicus*. *Plant Physiology* **137**, 1272-1282.
- Eckardt, N.A. (2006) Functional Divergence of AP3 Genes in the MAD World of Flower Development. *Plant Cell* **18**(8), 1779–1781.

- Ferrándiz, C., Navarro, C., Gómez, M.D., Cañas, L.A. and Beltrán, J.P.** (1999) Flower development in *Pisum sativum*: From the war of the whorls to the battle of the common primordia. *Developmental Genetics* **25**, 280-290.
- Ferrándiz, C., Gu, Q., Martienssen, R. and Yanofsky, M.F.** (2000) Redundant regulation of meristem identity and plant architecture by *FRUITFULL*, *APETALA1* and *CAULIFLOWER*. *Development* **127**, 725-734.
- Force, A., Lynch, M., Pickett, F.B., Amores, A., Yan, Y.L. and Postlethwait, J.** (1999) Preservation of duplicate genes by complementary, degenerative mutations. *Genetics* **151**, 1531-1545.
- Geuten, K. and Irish, V.** (2010) Hidden variability of floral homeotic B genes in Solanaceae provides a molecular basis for the evolution of novel functions. *The Plant Cell* **22**, 2562-2578.
- Goto, K. and Meyerowitz, E.M.** (1994) Function and regulation of the *Arabidopsis* floral homeotic gene *PISTILLATA*. *Genes & Development* **8**, 1548-1560.
- Hartweck, L.M., Scott, C.L. and Olszewski, N.E.** (2002) Two O-linked N-acetylglucosamine transferase genes of *Arabidopsis thaliana* L. Heynh. have overlapping functions necessary for gamete and seed development. *Genetics* **161**, 1279-1291.
- Heard, J. and Dunn, K.** (1995) Symbiotic induction of a MADS-box gene during development of alfalfa root-nodules. *Proceedings of the National Academy of Sciences of the United States of America* **92**, 5273-5277.
- Hecht, V., Foucher, F., Ferrandiz, C., Macknight, R., Navarro, C., Morin, J., Vardy, M.E., Ellis, N., Beltrán, J.P., Rameau, C. and Weller, J.L.** (2005) Conservation of *Arabidopsis* flowering genes in model legumes. *Plant Physiology* **137**, 1420-1434.
- Henschel, K., Kofuji, R., Hasebe, M., Sadler, H., Münster, T. and Theissen, G.** (2002) Two ancient classes of MIKC-type MADS-box genes are present in the moss *Physcomitrella patens*. *Mol Biol Evol* **19**, 801-814.
- Hewitt, Y.M.** (1966) Sand and water culture methods used in the study of plant nutrition. Farnham Royal, Bucks. Commonwealth Agricultural Bureaux.
- Honma, T., and Goto, K.** (2001) Complexes of MADS-box proteins are sufficient to convert leaves into floral organs. *Nature* **409**, 469-471.
- Hughes, A.L.** (1994) The evolution of functionally novel proteins after gene duplication. *Proceedings of the Royal Society of London Series B-Biological Sciences* **256**, 119-124.
- Irish, V.F.** (2006) Duplication, diversification, and comparative genetics of angiosperm MADS-box genes. *Advances in Botanical Research: Incorporating Advances in Plant Pathology* **44**:129-161.
- Jack, T., Brockman, L.L. and Meyerowitz, E.M.** (1992) The homeotic gene *APETALA3* of *Arabidopsis thaliana* encodes a MADS-box and is expressed in petals and stamens. *Cell* **68**, 683-697.
- Jack, T., Fox, G.L. and Meyerowitz, E.M.** (1994) Homeotic gene *APETALA3* ectopic expression. Transcriptional and post-transcriptional regulation determine floral organ identity. *Cell* **76**, 703-716.
- James, P., Halladay, J. and Craigies, E.** (1996) Genomic Libraries and a Host Strain Designed for Highly Efficient Two-Hybrid Selection in Yeast. *Genetics* **144**, 1425-1436.
- Kim, S.T., Yoo, M.J., Albert, V.A., Farris, J.S., Soltis, P.S. and Soltis, D.E.** (2004) Phylogeny and diversification of B-function MADS-box genes in angiosperms: Evolutionary and functional implications of a 260-million-year-old duplication. *American Journal of Botany* **91**, 2102-2118.
- Kramer, E.M., Dorit, R.L. and Irish, V.F.** (1998) Molecular evolution of genes controlling petal and stamen development: Duplication and divergence within the *APETALA3* and *PISTILLATA* MADS-box gene lineages. *Genetics* **149**, 765-783.
- Kramer, E.M. and Irish, V.F.** (2000) Evolution of the petal and stamen developmental programs: Evidence from comparative studies of the lower eudicots and basal angiosperms. *International Journal of Plant Sciences* **161**, S29-S40.
- Kramer, E.M., Di Stilio, V.S. and Schluter, P.** (2003) Complex patterns of gene duplication in the *APETALA3* and *PISTILLATA* lineages of the Ranunculaceae. *Int. J. Plant Sci.* **164**, 1-11.
- Kramer, E.M., Su, H-J., Wu, J.M. and Hu, J.M.** (2006) A simplified explanation for the frameshift mutation that created a novel C-terminal motif in the *APETALA3* gene lineage. *BMC Evol. Biol.* **6**, 30.
- Lamb, R.S. and Irish, V.F.** (2003) Functional divergence within the *APETALA3/PISTILLATA* floral homeotic gene lineages. *Proceedings of the National Academy of Sciences of the United States of America* **100**, 6558-6563.

- Liu, Y., Nakayama, N., Schiff, M., Litt A., Irish, V.F., and Dinesh-Kumar, S.P.** (2004) Virus induced gene silencing of a DEFICIENS ortholog in *Nicotiana benthamiana*. *Plant Mol. Biol.* **54**, 701-711.
- Lynch, M. and Force, A.** (2000) The probability of duplicate gene preservation by subfunctionalization. *Genetics* **154**, 459-473.
- Lynch, M. and Conery, J.S.** (2000) The evolutionary fate and consequences of duplicated genes. *Science* **290**, 1151-1155.
- Lynch, M., O'Hely, M., Walsh, B. and Force, A.** (2001) The probability of preservation of a newly arisen gene duplicate. *Genetics* **159**, 1789-1804.
- Ohno, S.** (1970) Evolution by Gene Duplication. Springer-Verlag, Heidelberg, Germany.
- Paez-Valencia, J., Sanchez-Gomez, C., Valencia-Mayoral, P., Contreras-Ramos, A., Hernandez-Lucas, I., Orozco-Segovia, A. and Gamboa-DeBuen, A.** (2008) Localization of the MADS domain transcriptional factor *NMH7* during seed, seedling and nodule development of *Medicago sativa*. *Plant Science* **175**, 596-603.
- Perbal, M.C., Haughn, G., Saedler, H., Schwarz-Sommer, Z.** (1996) Non-cell-autonomous function of the *Antirrhinum* floral homeotic proteins DEFICIENS and GLOBOSA is exerted by their polar cell-to-cell trafficking. *Development* **122**, 3433-3441.
- Pnueli, L., Abuabeid, M., Zamir, D., Nacken, W., Schwarz-Sommer, Z. and Lifschitz, E.** (1991) The MADS box gene family in tomato - temporal expression during floral development, conserved secondary structures and homology with homeotic genes from *antirrhinum* and *arabidopsis*. *Plant Journal* **1**, 255-266.
- Riechmann, J.L., Krizek, B.A. and Meyerowitz, E.M.** (1996) Dimerization specificity of Arabidopsis MADS domain homeotic proteins *APETALA1*, *APETALA3*, *PISTILLATA*, and *AGAMOUS*. *Proc. Natl. Acad. Sci. USA* **93**, 4793-4798.
- Rijkema, A.S., Royaert, S., Zethof, J., van der Weerden, G., Gerats, T. and Vandenbussche, M.** (2006) Analysis of the *Petunia TM6* MADS box gene reveals functional divergence within the *DEF/AP3* lineage. *Plant Cell* **18**, 1819-1832.
- Schwarz-Sommer, Z., Hue, I., Huijser, P., Flor, P.J., Hansen, R., Tetens, F., Lönnig, W.E., Saedler, H. and Sommer, H.** (1992) Characterization of the *Antirrhinum* floral homeotic MADS-box gene *DEFICIENS*. Evidence for DNA binding and autorregulation of its persistent expression throughout flower development. *Embo Journal* **11**, 251-263.
- Soltis, P.S., Brockington, S.F., Yoo, M.J., Piedrahita, A., Latvis, M., Moore, M.J., Chanderbali, A.S. and Soltis, D.E.** (2009) Floral variation and floral genetics in Basal Angiosperms. *American Journal of Botany* **96**, 110-128.
- Sommer, H., Beltán, J.P., Huijser, P., Pape, H., Lonning, W.E., Saedler, H. and Schwarz-Sommer, Z.** (1990) *DEFICIENS*, a homeotic gene involved in the control of flower morphogenesis in *Antirrhinum majus*. The protein shows homology to transcription factors. *Embo Journal* **9**, 605-613.
- Stellari, G.M., Jaramillo, M.A. and Kramer, E.M.** (2004) Evolution of the *APETALA3* and *PISTILLATA* lineages of MADS-box containing genes in basal angiosperms. *Mol. Biol. Evol.* **21**, 506-519.
- Szczyglowski, K. and Amyot, L.** (2003) Symbiosis, inventiveness by recruitment?. *Plant Physiology* **131**, 935-940.
- Tadege, M., Ratet, P. and Mysore, K.S.** (2005) Insertional mutagenesis: a Swiss army knife for functional genomics of *Medicago truncatula*. *Trends in Plant Science* **10**, 229-235.
- Tadege, M., Wen, J.Q., He, J., Tu, H.D., Kwak, Y., Eschstruth, A., Cayrel, A., Endre, G., Zhao, P.X., Chabaud, M., Ratet, P. and Mysore, K.S.** (2008) Large-scale insertional mutagenesis using the *Tnt1* retrotransposon in the model legume *Medicago truncatula*. *Plant Journal* **54**, 335-347.
- Tamura, K., Dudley, J., Nei, M. and Kumar, S.** (2007) MEGA4: Molecular evolutionary genetics analysis (MEGA) software version 4.0. *Molecular Biology and Evolution* **24**, 1596-1599.
- Taylor, S.A., Hofer, J.M.I., Murfet, I.C.** (2001) *Stamina pistilloida*, the pea orthologue of *Fim* and *UFO*, is required for normal development of flowers, inflorescences and leaves. *Plant Cell* **13**, 31-46.
- Theissen, G. and Melzer, R.** (2007) Molecular mechanisms underlying origin and diversification of the angiosperm flower. *Annals of Botany* **100**, 603-619.
- Tröbner, W., Ramirez, L., Motte, P., Hue, I., Huijser, P., Lonning, W.E., Saedler, H., Sommer, H. and Schwarz-Sommer, Z.** (1992) *GLOBOSA*, a homeotic gene which interacts with *DEFICIENS* in the control of *Antirrhinum* floral organogenesis. *Embo Journal* **11**, 4693-4704

- Tucker, S.C.** (1989) Overlapping organ initiation and common primordia in flowers of *Pisum sativum* (*Leguminosae papilionoideae*). *American Journal of Botany* **76**, 714-729.
- Tucker, S.C.** (2003) Floral development in legumes. *Plant Physiology* **131**, 911-926.
- Urbanus, S.L., de Folter, S., Shchennikova, A.V., Kaufmann, K., Immink, R.G.H. and Angenent, G.** (2009) In planta localisation patterns of MADS domain proteins during floral development in *Arabidopsis thaliana*. *BMC Plant Biol.* **9**, 5.
- Vandenbussche, M., Zethof, J., Royaert, S., Weterings, K. and Gerats, T.** (2004) The duplicated B-class heterodimer model: Whorl-specific effects and complex genetic interactions in *Petunia hybrida* flower development. *Plant Cell* **16**, 741-754.
- Van Der Krol, A.R. and Chua, N.H.** (1993) Flower development in *Petunia*. *Plant Cell* **5**, 1195-1203.
- Vincent, J.M.** (1970) A manual for the practical study of the root nodule bacteria. Oxford, England. IBP. Handbook . **15**. 164
- Wesley, S.V., Helliwell, C.A., Smith, N.A., Wang, M.B., Rouse, D.T., Liu, Q., Gooding, P.S., Singh, S.P., Abbott, D., Stoutjesdijk, P.A., Robinson, S.P., Gleave, A.P., Green, A.G. and Waterhouse, P.M.** (2001) Construct design for efficient, effective and high-throughput gene silencing in plants. *Plant Journal* **27**, 581-590.
- Wu, C.X., Ma, Q.B., Yam, K.M., Cheung, M.Y., Xu, Y.Y., Han, T.F., Lam, H.M. and Chong, K.** (2006) *In situ* expression of the *GmNMH7* gene is photoperiod-dependent in a unique soybean (*Glycine max* L. Merr.) flowering reversion system. *Planta* **223**, 725-735.
- Zuccherro, J.C., Caspi, M. and Dunn, K.** (2001) *ngl9*: A third MADS box gene expressed in alfalfa root nodules. *Molecular Plant-Microbe Interactions* **14**, 1463-1467.

Figure legends

Figure 1. Neighbor-Joining Tree of AP3-like MADS-box genes from a selection of diverse species. The numbers next to the nodes refer to bootstrap values from 1000 pseudo-replicates.

Figure 2. Expression patterns of *M. truncatula* AP3-like genes in different plant tissues. (a) Northern blot analysis of *MtNMH7* and *MtTM6* genes in different *M. truncatula* tissues. (b) Comparative expression analysis of the AP3-like MADS-box genes. The height of the bars for a given gene indicates relative differences in expression levels in floral buds. The highest expression value scored (*MtTM6*) was set to 1.00, and lower values were plotted relative to this highest value. N: nodules; R: roots; S: shoots; L: leaves; F: flowers.

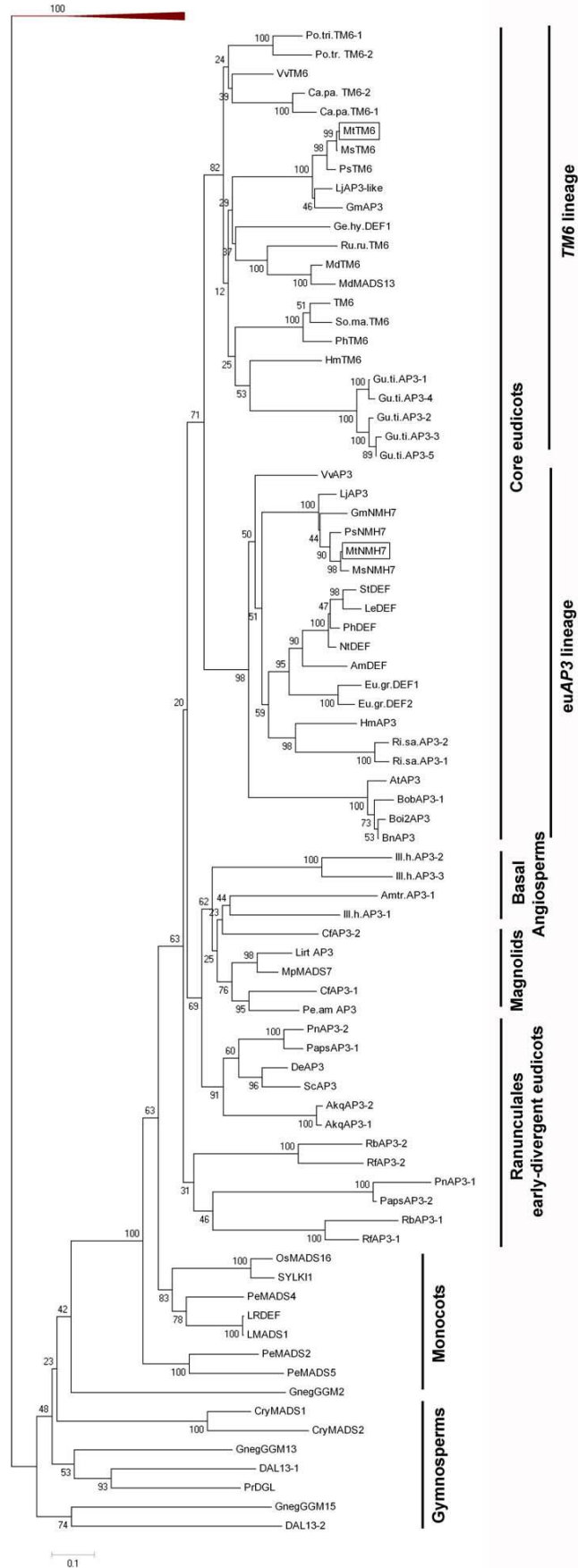
Figure 3. Expression patterns of the *M. truncatula* AP3-like genes during floral development. *In situ* hybridization of the *MtNMH7* and *MtTM6* mRNA in *M. truncatula* wild-type flower buds. Left: schematic diagram of the common primordia to petals and stamens present in some legume species and a flower bud of *M. truncatula* at stage 6 showing the petal and stamens developed from one of the four common primordia domains (purple area). Developmental stages were defined according to Benlloch *et al.*, 2003. (a) At stage 4, *MtNMH7* transcripts are located in the inner cell layers of the common primordia. (b) At stage 6, *MtNMH7* expression is found in the inner cell layers of the developing petals and stamens. The expression was not observed in the outer cell layers of these organs. (c) *MtNMH7* mRNA is detected at later stages of petal and stamen development with a similar spatial distribution. (d) Close view of a carpel showing the *MtNMH7* expression in the ovules. (e) At stage 4, *MtTM6* mRNA is strongly expressed in the most external cell layers of the common primordia and in the central region of the floral meristem. (f) At stage 6, *MtTM6* mRNA is only detected in the outer cell layers of petals and stamens. (g) At stage 7, *MtTM6* expression remains visible in the

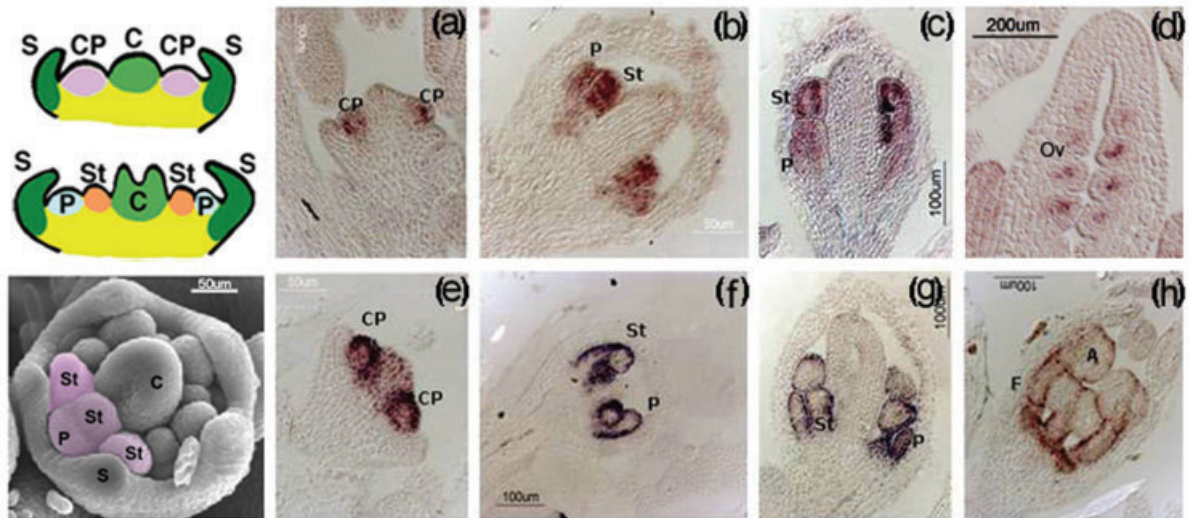
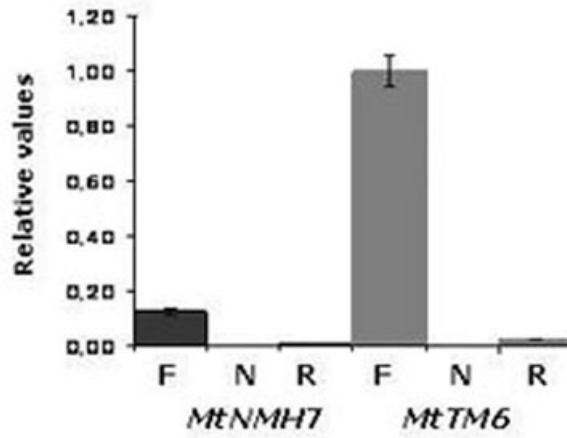
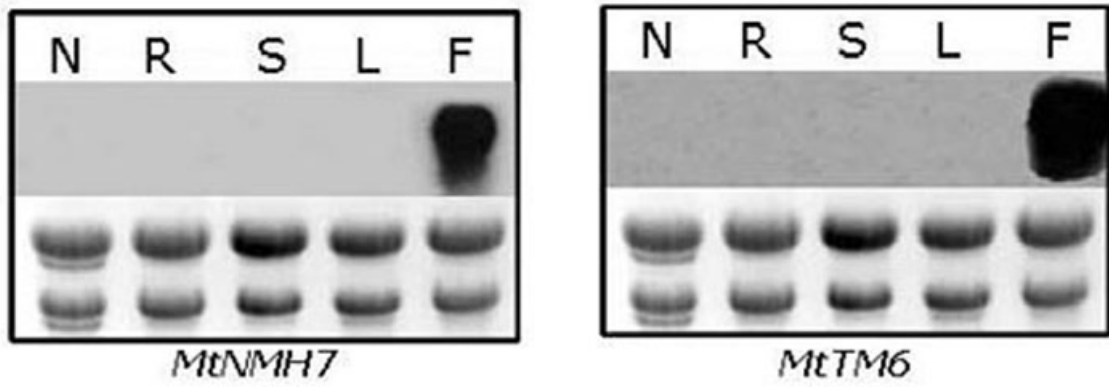
peripheral cells of petals and stamens. **(h)** Detailed view of the *MtTM6* expression pattern in the outer cell layers of anthers and filaments at later stages of floral development. CP: common primordia; P: petals; St: stamens; Ov: ovules; A: anthers; F: filaments.



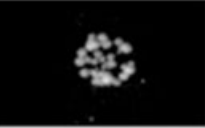
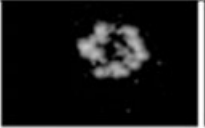

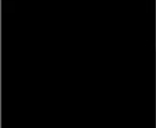
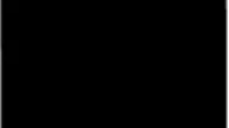
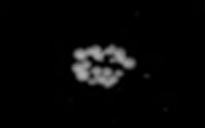
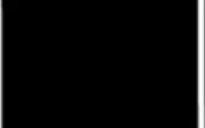











Figure 4. *M. truncatula* B-class MADS-box protein interactions evaluated by the yeast GAL4 Two-Hybrid assay. GAL4 BD-fused bait proteins and GAL4 AD-fused prey proteins were co-transformed into the PJ69-4A yeast strain. Interactions were detected by the ability to grow in minimal medium lacking adenine and histidine (SD-L-W-H-A). BD: GAL4 binding domain; AD: GAL4 activation domain.

Figure 5. Phenotypic effects of the 35S::RNAi-MtNMH7 and 35S::RNAi-MtTM6-mttm6-1 on *M. truncatula* flowers. **(a)** Dissected wild-type *M. truncatula* flower showing normal petals in W2: vexillum or standard (V), wings (W), keel (K) and staminal tube (ST) with fused filaments and anthers (W3) surrounding the central carpel (C, W4). **(b)** 35S::RNAi-MtNMH7 flower. The W2 contains petals with sepal-like (green) mosaic tissues (white arrows). W3 contains several stamens with partial homeotic transformation into carpel-like structures. The two stamens flanking the staminal tube showed atypical filaments and green carpelloid anthers (white arrows). **(c)** *mttm6-1* flower. The W2 contains petals with green tissues distributed in small areas and, occasionally, a carpel-like structure is fused to a petal (white arrows). The W3 is occupied by carpel-like structures. **(d)** 35S::RNAi-MtTM6 flower. The W2 was affected only in terms of petal shape. The W3 contains several stamens with partial homeotic transformation into carpel-like structures which are not fused to form the staminal tube (white arrow). Some anthers end in a structure that resembles a stigma.

Figure 6. Scanning electron microscopy (SEM) analysis of cellular types in whorls 2 and 3 of the 35S::RNAi-MtNMH7 and *mttm6-1* flowers. Adaxial epidermal cells of a wild-type petal. **(b)** Adaxial epidermal cells of a wild-type sepal. **(c)** Adaxial view of a 35S::RNAi-MtNMH7 sepal-like mosaic organ in W2. Neighboring cells show conical and striated cells characteristics of wild-type petals. **(d)** A small fraction of cells in the W2 of *mttm6-1* flowers have become typical sepal cells, while other neighboring cells maintain the typical striations of petal cells but have lost their characteristic conical shape. **(e)** Cells of a wild-type filament. **(f)** Cells of the low and middle wild-type carpel **(g)** Cells of the filament in 35S::RNAi-MtNMH7 carpelloid stamens. **(h)** Cells of the middle section of the *mttm6-1* carpelloid stamens. **(i)** Cells of the wild-type anthers. **(j)** Cells of the wild-type ovules. **(k)** Cells of the ovule-like structures in W3 of the 35S::RNAi-MtNMH7 flowers. **(l)** Cells in the top of the wild-type carpel. **(m)** *mttm6-1* carpelloid stamen. **(n)** Wild-type stamens fused in a staminal tube. **(o)** 35S::RNAi-MtNMH7 weakly carpelloid stamens. **(p)** Wild-type carpel. **(q)** *mttm6-1* carpelloid stamens.





BD/AD	AD-MtPI	AD-MtNGL9	AD-MtNMH7	AD-MtTM6	AD
BD-MtPI					
BD-MtNGL9					
BD-MtNMH7					
BD-MtTM6					
BD	